Comparison of analytical and numerical solutions for stresses and displacements around unlined tunnels with arbitrary cross sections inside anisotropic rock masses

Manuel Bernhard Winkler
Graz University of Technology, Institute of Rock Mechanics and Tunnelling, Graz, Austria

Ali Yaz
Istanbul Technical University, Istanbul, Turkey

Thomas Marcher
Graz University of Technology, Institute of Rock Mechanics and Tunnelling, Graz, Austria

ABSTRACT: The implementation of closed-form solutions for stress and displacement fields around tunnels with arbitrary geometry, often based on the complex variable theory and the method of conformal mapping, can be quite challenging from a mathematical point of view. In this paper a solution strategy for the implementation of a chosen closed-form solution from literature is presented, including the possibility to account for rock mass anisotropy and arbitrary tunnel geometries. The evaluation of the involved elastic potential functions is described, respectively derivatives thereof, in terms of solving non-linear constrained optimization problems. To validate our approach, the analytical results for stresses and displacements around a tunnel with semicircular geometry are compared to numerical results from finite element computations. The outcome of the study should be regarded as a basis for the development of refined analytical solutions within anisotropic rock masses considering more realistic boundary conditions and effects such as material non-linearity.

Keywords: analytical solution, complex variable theory, conformal mapping, tunnel displacements, non-linear optimization problem, transverse isotropic rock mass.

1 INTRODUCTION

For the derivation of closed-form planar elasticity solutions for stress and displacement fields around arbitrarily shaped tunnels in isotropic or anisotropic grounds the complex variable theory, as initiated by Kolosov (1909), in combination with the conformal mapping method (Muskhelishvili 1953) can be used. Thereby, the exterior of the original problem configuration is mapped to the outside or inside of a fictitious unit circle. Despite the complexity of the involved mapping procedure, the associated difficulties are outweighed by the simpler definitions of the elastic potential functions influencing the amount of generated stresses and displacements.

One elastic closed-form solution based on the complex variable theory and the method of conformal mapping is the solution by Tran Manh et al. (2015). It accounts for arbitrary tunnel shapes and elastic rock mass anisotropy by the assumption over transverse isotropy. Mathematical optimization problems need to be solved in the course of determining the elastic potential functions, which is not a straightforward process. Consequently, in this paper a solution strategy to overcome such difficulties in connection with complex variable solutions is provided. The assumption is made that the mapping coefficients of the conformal mapping function are already known, e.g. from an iterative scheme as presented by Winkler et al. (2023). Finally, the solutions for stresses and displacements of a specific case are compared with the results from finite element calculations. Section 2 refers to the problem definition. In section 3 the solution procedure for the determination of the derivatives of the elastic potentials and the retrieval of the final solutions are described. In section 4 the analytical solution is compared against results from finite element computations and section 5 presents the conclusions.

2 PROBLEM DEFINITION

In the solution of Tran Manh et al. (2015) the initial problem consists of a tunnel with an arbitrary geometry (in our case semicircular) excavated in an infinite elastic and transversely isotropic rock mass. The planes of isotropy are oriented at an angle β from the horizontal x^* – axis along the local x'-y'- coordinate system in the original configuration (see Figure 1a). The initial stresses are assumed to be homogeneous and anisotropic with a vertical stress σ_0 and a horizontal stress $K_0 \cdot \sigma_0$. The far-field stresses σ_{v0}, σ_{h0} and τ_{vh} follow a rotation of the planes of isotropy to the horizontal direction by the angle β. The rotated configuration (x-y-system), later referred to as the z-plane, is the configuration considered for the conformal mapping and the evaluation of the elastic potentials.

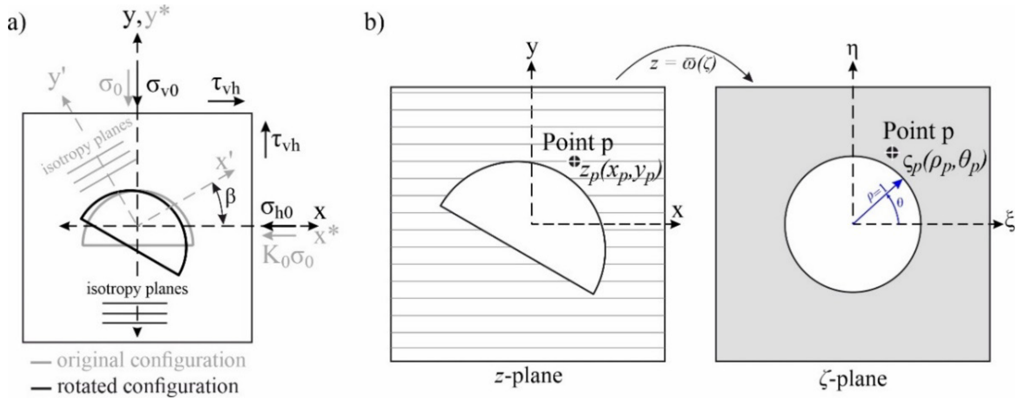

Figure 1. a) Problem consideration and coordinate systems for the original configuration and the rotated configuration (after Tran Manh et al. 2015) and b) Conformal mapping of points from the physical z-plane onto the unit circle exterior in the ζ –plane .

In Fig 1b) the mapping process of points from the z-plane to the exterior of a unit circle on the ζ-plane is shown. In the solution of Tran Manh et al. (2015), the mapping of points p on the tunnel exterior in the z-plane, expressed in terms of the complex variable $z_p = x_p + iy_p$, is carried out to the outside of a unit circle (p expressed as $\zeta_p = \rho_p e^{i\theta p}$ with polar radius ρ_p and polar angle θ_p) based on the negative powers of the Laurent series (Eqn.1). In Eqn. (1) N represents the number of terms used in the series expansion. Higher values for N increase the mapping accuracy (here 3 is chosen). R is a constant mapping factor (size related) and M_n are the constant mapping coefficients (shape related). R and M_n are assumed to be already known in this study.

$$z = \varpi(\zeta) = R\left[\zeta + \sum_{n=1}^{N} M_n \zeta^{-n}\right] \tag{1}$$

The elastic potential U for transversely isotropic bodies in plane "hole-in-plate" elasticity problems, from which the solutions for stresses are derived, can be expressed by two analytical potential functions $\Omega_1(z_1)$ and $\Omega_2(z_2)$ and their conjugates depending on the complex variables z_1 and z_2 (Green & Zerna 1954).

$$z_k = z + \gamma_k z^* \quad (k = 1{,}2) \tag{2}$$

with superscript * indicating the complex conjugate of z and γ_k representing a derived material constant related to the anisotropic elastic parameters defined with respect to the local x'-y'-system. The final aim of the solution procedure is to determine the first and second order derivatives of the potential functions as they appear in the final solutions for the stresses and displacements. Detailed formulae for any derived material constants and the required derivatives of potentials Ω_1 and Ω_2, as included in the final equations for stresses and displacements, are given in Tran Manh et al. (2015).

3 SOLUTION PROCEDURE

3.1 Mapping from z_k-planes to ζ_k-planes

The derivatives of the potentials Ω_k ($k = 1, 2$), as part of the equations for stresses and displacements stated in Tran Manh et al. (2015), are defined as functions of points ζ_k on the ζ_k –planes corresponding to points z_k on the z_k-planes. Therefore, in a first step points ζ_k need to be determined from points z_k.

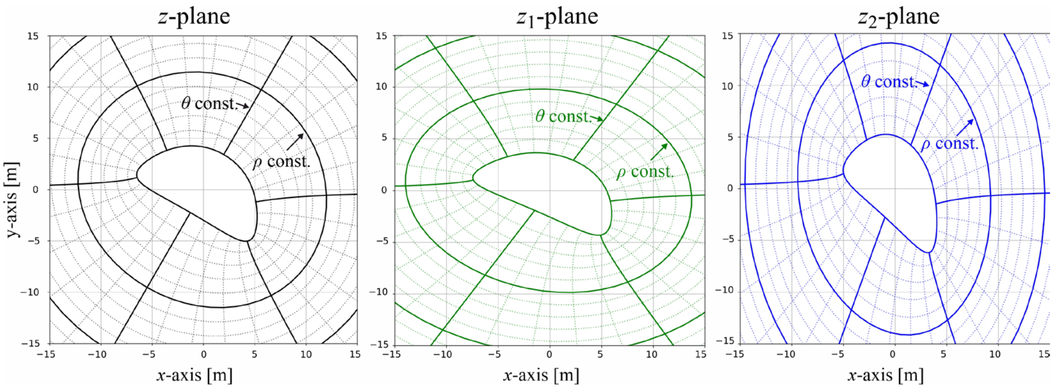

Figure 2. Representation of closed lines associated with constant values θ and radial lines associated with constant values ρ from the ζ-plane in the tunnel exterior within planes z, z_1 and z_2.

Figure 2 depicts a graphical representation of the tunnel exterior on planes z and z_k, by displaying mapped groups of points with constant radius ρ or constant polar angles θ from the ζ-plane using Eqns. (1) and (2) and taking into account the known mapping coefficients.

It is noticeable from this figure that parameter γ_k fictively yields a stretching, respectively squeezing, of the medium as compared to the z-plane. This enables taking into account the effects of transverse isotropy in a subsequent step when the elastic potentials $\Omega_k(z_k(\zeta_k))(k = 1{,}2)$, respectively derivatives thereof, are computed for single discrete points ζ_k on the corresponding unit circle domains (ζ_k - planes).

In order to evaluate points ζ_k, a mapping relation between discrete points ζ_k and z_k as stated in Eqn. (7) can be set up by plugging Eqn. (1) into Eqn. (2) and applying some mathematical simplifications.

$$z_{k,map} = R \sum_{n=1}^{N} c_{kn}{\zeta_k}^{n} + d_{kn}{\zeta_k}^{-n}, \text{for } k = 1{,}2 \tag{3}$$

with $c_{k1} = 1+\gamma_k M_1^*$, $d_{k1} = M_1+\gamma_k$ and $c_{kn} = \gamma_k M_n^*$ and $d_{kn} = M_n$ for n ≥2. Each discrete point $\zeta_{l,k} = \rho_{l,k}e^{i\theta_{l,k}}$ (l = 1 to number of discrete points in z_k-plane) corresponding to a known discrete point $z_{l,k} = x_{l,k}+iy_{l,k}$ is determined by solving a non-linear constrained optimization problem defined as

$$\min f(\rho_{l,k},\theta_{l,k}) = \sqrt{\left(R_e\left[z_{l,k} - z_{l,k,map}(\rho_{l,k},\theta_{l,k})\right]\right)^2 + \left(I_m\left[z_{l,k} - z_{l,k,map}(\rho_{l,k},\theta_{l,k})\right]\right)^2}$$
$$\text{s.t.}\ \sqrt{\left(\rho_{l,k}\cos\theta_{l,k}\right)^2 + \left(\rho_{l,k}\sin\theta_{l,k}\right)^2} \geq 1\ \text{(unit circle exterior)} \tag{8}$$

In order to solve the above stated problem, any of the available non-linear constrained minimization routines can be used. In this study, the *SLSQP* (Sequential Least Squares Programming) algorithm as part of Phyton's `scipy.optimize` module (Jones et al.) is applied to solve for unknown points ζ_k.

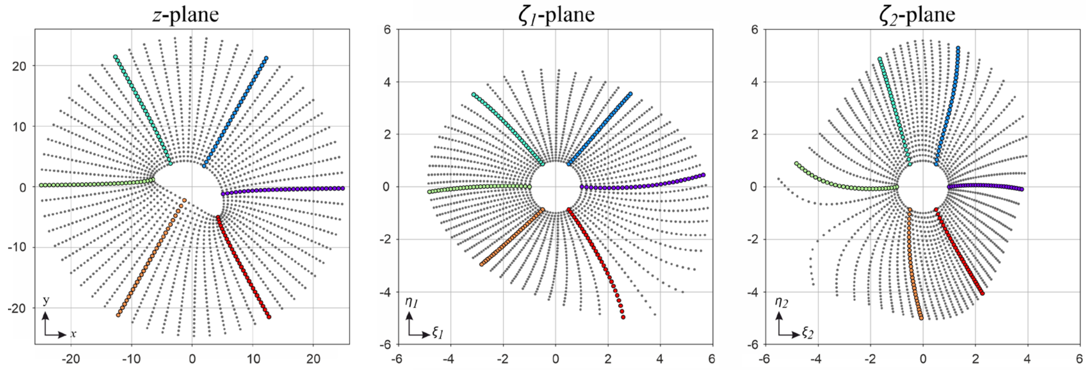

Figure 3. Representation of associated points on the tunnel exterior within planes z, ζ_1 and ζ_2.

The points ζ_k are subsequently used for the computation of the required first and second order derivatives of the stress potentials Ω_k, as part of the final equations (Tran Manh et al. 2015) for stresses and displacements arising from the tunnel excavation. To correspond these calculated quantities to physical locations of points in the rock mass, they are assigned to points z in the z-plane that were originally computed (Eqn. 1) from the same discrete points ζ, with polar coordinates ρ and θ, as the points z_k on the z_k-planes using Eqn. (2). Figure 3 shows optimized point locations on the ζ_k-planes corresponding to the associated points on the z-plane. Equally colored points on the shown planes, different from black, show points with constant polar angles θ from the ζ-plane.

3.2 *Final solutions*

Once the derivatives of the stress potentials Ω_k, are found for each point on the z-plane, the stress and displacement field changes arising from the relaxation of the internal pressure by a stress release factor λ can be determined using formulae presented in the paper of Tran Manh et al. (2015). To receive the final stress field for the given problem in the rotated configuration (see Figure 1a) the computed changes in the stresses must be superimposed on the initial values for the stress components. In a final step, the whole system, including the geometry and the stress and displacement fields must be rotated back into the original configuration.

4 RESULTS

To validate the implemented analytical solution a numerical finite element model was set up in Plaxis2D (PLAXIS Reference Manual: 2D - Connect Edition V22). A semicircular tunnel with radius R = 6.5 m was studied. The jointed rock constitutive model with a transversely isotropic stiffness formulation was employed to model the elastic anisotropic response of the rock mass. Any plastification of the continuum was prevented by setting the strength parameters to artificially high values. A homogenous initial stress field without any stress gradients was taken into account. The initial vertical stress component was assumed with a value of σ_0 = 5.25 MPa. A K_0-coefficient of K_0 = 0.75 was applied to model the initial horizontal stresses. The computation was carried out for a full relaxation of the internal pressure (λ=1.0) and the orientation of the planes of isotropy was modelled at an angle β=30° from the horizontal axis. The elastic parameters of the rock mass and the values for the mapping coefficients (rotated configuration) were considered as given in Table 1.

Table 1. Elastic parameters of the rock mass and considered mapping coefficients for the validation case

Parameter	Unit	Symbol	Value	Mapping Coefficients (Rotated Configuration)
Young's modulus	[MPa]	$E_{y'}$	10500	$R = 4.952 - 0.00i$
Poisson's ratio	[-]	$\nu_{y'x'}$	0.3	$M_1 = 0.1541 - 0.2676i$
Young's modulus	[MPa]	$E_{x'}$	15800	$M_2 = -0.1394 - 0.0010i$
Poisson's ratio	[-]	$\nu_{x'z'}$	0.3	$M_4 = 0.0168 + 0.0272i$
Shear modulus	[MPa]	$G_{y'x'}$	3950	

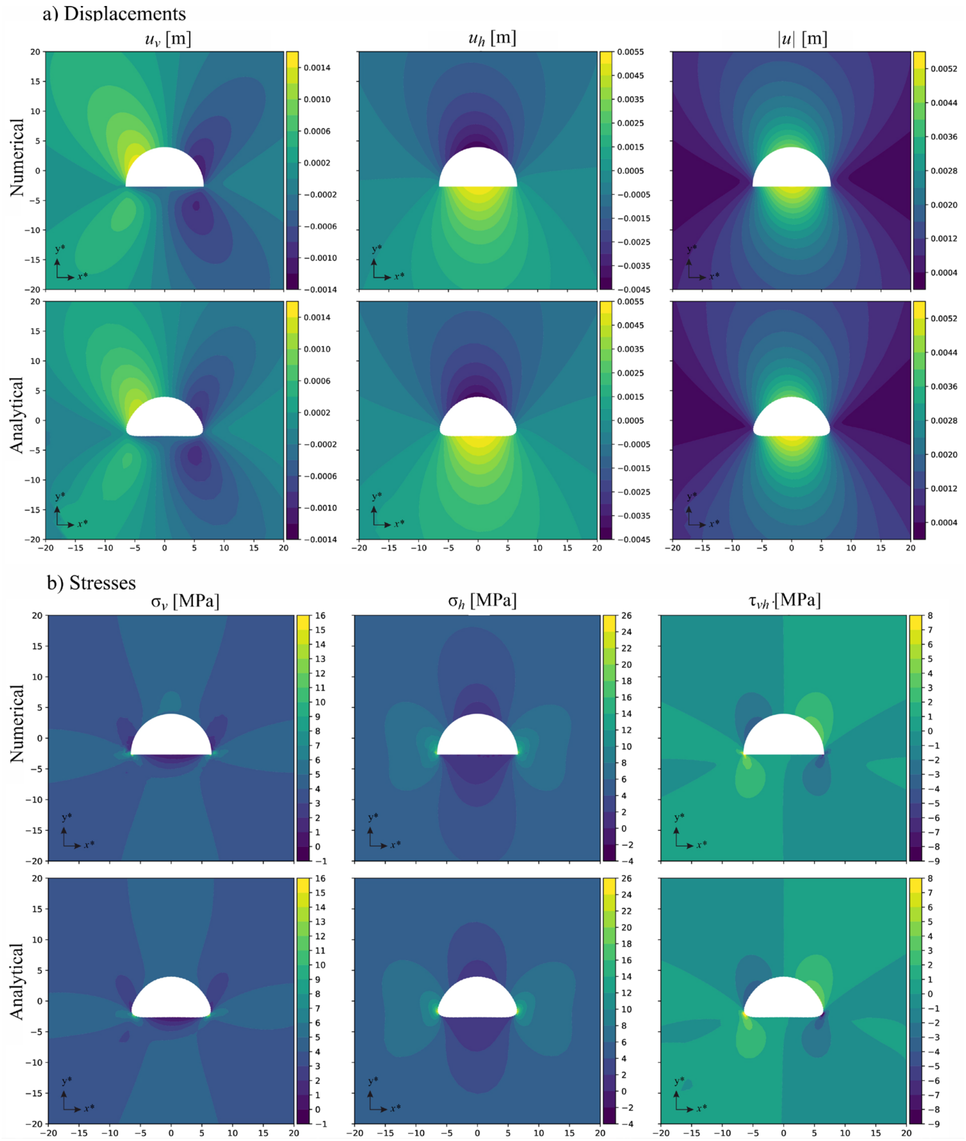

Figure 4. Contour plots for resulting a) displacements and b) stresses from the numerical and analytical solutions in the x^*-y^*-coordinate system.

Figure 4 compares the numerical and analytical results in terms of contour plots of displacements and stresses in the global Cartesian system (original configuration acc. to Figure 1). Overall, a very good agreement between the results from both calculation approaches can be seen. Any visual differences are attributed to the approximation of the geometry and the domain discretization density in the analytical solution. Further, the numerical solutions might slightly be influenced by boundary effects, from the fixation of the deformation boundaries, and/or the density of the finite element mesh. However, a sensitivity study on the influence of the mesh density on the results from the finite element solution was not carried out.

5 CONCLUSION AND OUTLOOK

An implementation strategy for an analytical elastic transversely isotropic solution by Tran Manh et al. (2015) for stress and displacement fields in the exterior of unlined tunnels with arbitrary geometry based on the theory of complex variables in 2D has been presented.

A procedure for the determination of the tunnel exterior point locations on the k^{th} unit circle planes, as required for the computation of the elastic stress potentials, has been proposed connected with the solution of corresponding non-linear constrained optimization problems. The solution of the final results has been stated to follow from a superposition of the initial (stress) state and a back rotation of the rotated system into the system with an original orientation of the planes of isotropy. The suggested solution procedure has been verified by comparing the results of the closed-form solution to the results of a numerical finite element simulation. For the given boundary value problem both approaches resulted in the same magnitude and similar distribution of stresses and displacements over the tunnel exterior.

In future, the presented procedure can be applied to more complex closed-form solutions based on the complex variable theory and the method of conformal mapping. It can be extended to include possibilities for the consideration of tunnel supports, material non-linearity or the interaction of multiple tunnel tubes. Possible fields of applications are shape and lining optimizations in the course of tunnel designs and the back analysis of lining stresses based on tunnel deformational data and geometry data from laser scanning profiles.

REFERENCES

Green, A. E., & Zerna W. 1954. *Theoretical Elasticity*. Oxford, England: Claredon Press (1st published).

Jones, E., Oliphant, T., & Peterson, P. SciPy: Open Source Scientific Tools for Python. Retrieved from http://www.scipy.org/ (accessed on 18th January 2023)

Kolosov, G. V. 1909. *On an application of complex function theory to a plane problem of the mathematical theory of elasticity (in Russian)* (Doctoral Thesis). Yurev University, Yurev.

Muskhelishvili, N. I. 1953. *Some Basic Problems of the Mathematical Theory of Elasticity* (J.R.M. Radok, Trans.). Groningen: Noordhoff.

PLAXIS Reference Manual: 2D - Connect Edition V22. Retrieved from https://communities.bentley.com/cfs-file/__key/communityserver-wikis-components-files/00-00-00-05-58/PLAXIS2DCEV22.01_2D00_2_2D00_Reference.pdf (accessed 19 January 2023)

Tran Manh, H., Sulem, J., & Subrin, D. 2015. A Closed-Form Solution for Tunnels with Arbitrary Cross Section Excavated in Elastic Anisotropic Ground. *Rock Mechanics and Rock Engineering*, *48*(1), 277–288. https://doi.org/10.1007/s00603-013-0542-0

Winkler, M. B., Marcher, T., Yaz, A. 2023. An iterative scheme for the determination of the conformal mapping coefficients used in closed-form solutions for tunnels with arbitrary geometry. In: *Proceedings of the 15th ISRM International Congress on Rock Mechanics*, Schubert, W. & Kluckner, A. (eds), Salzburg, Austria, October 9 – October 13, 2023.